Bioorganic & Medicinal Chemistry Letters 20 (2010) 69–73

Contents lists available at ScienceDirect

Bioorganic & Medicinal Chemistry Letters

journal homepage: www.elsevier.com/locate/bmcl

Development of an in silico model for human skin permeation based on a Franz cell skin permeability assay

Pil H. Lee [a], Robert Conradi [b], Veerabahu Shanmugasundaram [a,*]

[a] Computer-Assisted Drug Discovery, Dynamics and Metabolism, Michigan Laboratories, Pfizer Global Research and Development, 2800 Plymouth Rd., Ann Arbor, MI 48105, United States

[b] Pharmacokinetics, Dynamics and Metabolism, Michigan Laboratories, Pfizer Global Research and Development, 2800 Plymouth Rd., Ann Arbor, MI 48105, United States

ARTICLE INFO

Article history:
Received 15 September 2009
Revised 6 November 2009
Accepted 10 November 2009
Available online 14 November 2009

Keywords:
Skin permeability
In silico
Computational
Franz cell
QSAR
Dermatology
Model

ABSTRACT

A multiple linear regression QSAR model was developed based on a set of 61 compounds with internally consistent permeability data measured across Franz cell. The data was normalized using a mean permeability value of a reference compound, 3-isobutyl-1-methylxanthine (IBMX). The QSAR model contained only five simple descriptors and had a correlation coefficient, r^2 of 0.77 between experimental and calculated values for skin permeability. The mean absolute error (MAE) was 0.3 for the entire set and the cross validation coefficient, q^2 was 0.71. The in silico skin permeability model was used as a filter for virtual libraries and to optimize skin permeation of specific compounds for several dermatology discovery projects.

The development of mathematical models to describe and predict skin permeability has been an area of active research.[1–3] The hair follicle, hair shaft and sebaceous gland collectively form what is called the pilosebaceous unit. Emerging interest in the pilosebaceous unit as a potential drug delivery target for a variety of dermatological conditions has accelerated a greater understanding of the structure and function of this unit as well as the design of drugs that selectively target hair follicles and sebaceous glands.[4–9] Stratum corneum, located on the outer surface of the skin, is a non-living layer of keratin-filled cells surrounded by a lipid-rich extracellular matrix that provides the primary barrier to drug delivery into skin.[10] In humans, it consists of between 10 and 25 layers of dead, elongated, fully keratinized corneocytes that are embedded in a matrix of lipid bilayers.[11] This layer is only 7–16 μm thick in most regions of the body but 400–600 μm thick in the palms of the hands and soles of the feet.[12] The stratum corneum consists of ~40% protein of which 80% is keratin. The type and amount of lipid in the stratum corneum depends on body-site and currently, it is generally accepted that skin permeability is affected by stratum corneum lipids.[13]

A number of skin permeability models, especially for predicting permeability of the stratum corneum to hydrophobic drugs have been proposed.[3,14,15] These models can be categorized into quantitative structure–property relationships (QSPRs), models based on diffusion mechanisms, or a combination of both.[1,2,16] One equation, developed by Potts and Guy,[3] correlates skin permeability (K_P) to a drug in aqueous solution with solute molecular weight (MW) and octanol–water partition coefficient (K_{oct}) given by Eq. 1:

$$\log K_p\ (\mathrm{cm/s}) = -6.3 + 0.71 * \log K_{oct} - 0.0061 * MW \qquad (1)$$

Similar equations have been proposed by other investigators,[17,18] parameters such as hydrogen bonding[19,20] and melting point have also been added to better fit the data. Other methods for estimating skin permeability include group contribution approaches[21] as well as combinations of molecular orbital calculations with neural networks[22] and random-walk calculations.[23] Additional models have been proposed to explain the size-dependence of skin permeation.[24]

Several of these published in silico models and structure–property relationships governing skin permeation are based on data gleaned from multiple sources using inconsistent experimental protocols.[16,25,26] The majority of these rely on the Flynn data set.[27] This compilation comprises data derived from at least 12 sources, on 93 solutes, only about half of which are drug-like molecules. This, along with the inherent variability of skin barrier properties, results in models of limited applicability to prospective

* Corresponding author at present address: Antibacterial Computational Chemistry, Groton Structural Biology, Worldwide Medicinal Chemistry, Pfizer Global Research and Development, Groton, CT-06340, United States. Tel.: +1 860 686 9264.
E-mail address: Veerabahu.Shanmugasundaram@pfizer.com.

0960-894X/$ - see front matter © 2009 Elsevier Ltd. All rights reserved.
doi:10.1016/j.bmcl.2009.11.039

dermal drug design. Large internally consistent data sets are hard to obtain, because skin permeation studies are so labor intensive. This difficulty is compounded by the necessity of using multiple skin sources per solute to average out permeability differences. Furthermore the vehicle used for skin permeability experimental studies in most published models is water. While a 100% aqueous vehicle is the most appropriate standard state, such a vehicle does not represent what is typical in topical discovery project applications. Furthermore, many drug-like solutes are too insoluble in pure water for it to be used as vehicle. Here we present both the generation of a consistent dataset used in our discovery efforts as well as the use of this dataset to derive a quantitative permeability model. The model was used to prioritize compounds to be tested in the Franz cell skin permeability assay, as a computational filter for virtual library design and in the optimization of skin permeability of compounds in several dermatology projects.

A set of 61 compounds with measured permeability values in Franz cell was gathered. The experimental permeability data was normalized using a mean value of the permeability of a reference compound, 3-isobutyl-1-methylxanthine (IBMX). The experimental data and calculated descriptors for 44 non-proprietary compounds out of 61 compound dataset are shown in Table 1. The normalized permeability (P_e) values for 61 compounds range from 2.4 to 9840 in 10^{-10} cm/s. The distribution of the permeability values for 61 compounds is shown in Figure 1, where the *x*-axis represents the $\log P_e$ and the *y*-axis represents the number of compounds. 3D conformations of compounds were generated using CORINA 3.1.[28] A variety of 2D/3D molecular descriptors were initially calculated. An initial correlation analysis of permeability values with four simple commonly used descriptors ($\log D$ at pH 6.5, $C \log P$,[29] topological polar surface area[30] (TPSA) and the number of rotatable bonds) was performed to obtain some trends from the dataset. Multiple linear regression modeling by JMP5.0.1.2[31] was performed using descriptors computed from QikProp 2.1.[32] The models were cross-validated 1000 times by leaving 20% of the data out. To assess the confidence of the predicted values from the model, we also calculated the 95% confidence interval for the predicted values. The confidence limits reflect variation in the error and variation in the parameter estimates. The confidence limits in JMP are calculated as described in Tan and Iglewicz.[33]

As discussed in the references and notes section,[34] to increase throughput, we performed skin permeation studies with cassettes of solutes (N in 1). Solute–solute interactions were reduced by keeping the concentrations of individual solutes at 0.1% or less and by using a mixed aqueous–organic vehicle to simultaneously reduce hydrogen bonding and solvophobic interactions between

Table 1
Experimental and computed permeability data (in cm/s) for 44 compounds in the Franz cell dataset and their corresponding computed properties

Compound name	$\log P_e$ (expt)	$\log P_e$ (pred)	PISA[a]	donorHB[a]	accptHB[a]	glob[a]	EA(eV)[a]	MW	$C \log P$	#rotor	$\log D$	TPSA
Sulfasalazine	−1.31	−1.42	406.547	2	9.25	0.7982147	1.805	398.3925	3.88	6	0.05	141.31
Sulfapyridine	−1.72	−1.62	300.312	2.5	6.5	0.8777503	0.085	249.2889	0.836	3	0.03	85.08
Tolbutamide	−0.04	0.42	122.775	1	3.5	0.8277124	0.424	270.3479	2.497	5	0.63	75.27
Testosterone	0.64	−0.02	29.538	1	3.7	0.9132449	0.072	288.4244	3.409	0	3.48	37.3
Hydrocortisone	−1.77	−1.74	28.542	3	8.15	0.9008329	0.046	362.4599	1.887	2	1.43	94.83
Progesterone	1.08	0.33	28.928	0	4	0.9008049	0.072	314.4617	3.965	1	4.04	34.14
Chlorpromazine	0.01	0.57	241.489	0	2.5	0.8577716	0.389	318.8642	5.3	4	2.15	6.48
Corticosterone	−0.89	−1.16	28.42	2	7.4	0.8910925	0.026	346.4605	2.513	2	1.76	74.6
Chlorthiazide	−2.15	−1.91	119.605	3	10	0.8911785	1.625	295.7232	−0.294	1	−0.78	118.69
Hydrochlorthiazide	−2	−1.73	68.84	3	9	0.8890697	0.953	297.7391	−0.365	1	−0.07	118.36
Dexamethasone	−2.4	−1.72	81.149	3	8.15	0.8924881	0.363	392.461	1.785	2	1.87	94.83
Indomethacin	−0.4	−0.3	203.376	1	5.75	0.8571297	1.085	357.7877	4.18	5	0.59	68.53
Caffeine	0.14	0.09	58.653	0	5	0.9056124	0.42	194.1906	−0.04	0	−0.13	61.82
Warfarin	−0.62	−0.58	338.631	1	5.25	0.8691987	0.976	308.3279	2.901	4	1.43	67.51
Propranolol hcl	−0.85	−0.4	264.835	2	3.95	0.8349111	0.399	259.3434	2.753	6	0.51	41.49
Furosemide	−1.41	−2.01	217.142	4	8	0.8573476	0.822	330.7441	1.27	5	−1	122.63
Lidocaine	0.25	−0.25	125.828	1	4.5	0.8684517	−0.239	234.3372	1.954	5	0.75	32.34
Carbamazepine	0.18	−0.35	321.304	2	2	0.8921892	0.517	236.2685	2.38	1	2.67	46.33
Clonidine hcl	−0.68	−0.11	133.205	2	2.5	0.8836365	0.133	230.0939	1.428	1	0.37	36.42
Piroxicam	−0.96	−1.02	322.19	1	7.75	0.8602271	1.257	331.3463	1.888	2	−0.35	99.6
Verapramil	−0.36	0.07	93.74	0	6.5	0.8146655	0.022	454.6017	4.466	13	1.52	63.95
Antipyrine	−0.15	−0.04	221.454	0	4	0.8966288	0.175	188.2257	0.204	1	0.27	26.93
Sulpiride	−1.48	−1.61	65.956	3	9.75	0.8255984	0.68	341.4258	1.11	6	−2.15	101.73
Niflumic acid	−0.27	0.32	265.405	1	2.5	0.854908	0.899	282.2179	4.922	3	2.01	62.22
Ketoprofen	−0.31	−0.24	276.938	1	4	0.8713042	0.623	254.2805	2.761	4	0.56	54.37
Ibmx	0	−0.25	67.56	1	5	0.9027192	0.458	222.2437	1.423	2	1.23	72.68
Desoximetasone	−1.28	−1.26	79.777	2	7.4	0.8883517	0	376.4616	2.591	2	1.85	74.6
5-Hydroxyquinoline	0.04	0.02	268.998	1	1.75	0.9305986	0.778	145.158	2.077	0	1.46	33.12
Metoprolol	−0.6	−0.59	124.886	2	5.65	0.8196366	−0.222	267.3639	1.486	9	−0.81	50.72
Ar–ligand-1	1.21	0.67	238.155	0	3	0.8484493	0.974	305.2977	4.001	3	5.59	39.92
Omeprazole	−1.02	−0.85	174.947	1	8	0.8471424	0.635	345.4161	2.565	5	2.16	77.1
Terbutaline	−1.68	−1.08	105.547	4	4.2	0.864664	0.075	225.2841	0.482	3	−2.14	72.72
Ru-58841	−0.06	−0.12	85.878	1	6.7	0.8332817	1.159	369.3384	1.214	5	2.41	84.64
Ar–ligand-2	0.53	0.39	263.742	1	2.25	0.8680521	1.21	263.2146	3.553	1	3.63	44.02
Sant-1	−0.01	−0.37	399.495	0	6.5	0.791687	0.378	373.494	4.424	5	3.65	36.66
Chloramphenicol	−1.17	−0.99	115.703	3	6.9	0.8589177	1.494	323.1293	1.283	6	1.02	112.7
Terfenadine	−0.92	−0.65	415.62	2	4.45	0.7730475	−0.178	471.6735	6.073	8	3.72	43.7
Rac	−0.34	−0.38	269.381	1	4.5	0.8670923	0.411	202.2093	1.766	2	1.22	55.13
Fexofenadine	−1.1	−1.42	412.65	3	6.45	0.7638154	−0.127	501.6564	1.957	10	2.3	81
Minoxidil	−1.41	−1.37	46.721	4	5.2	0.8862994	−0.122	209.2483	−2.134	1	−3.99	91.16
Miconazole	0.05	0.33	310.88	0	3.7	0.8333611	0.629	416.1286	5.812	6	5.55	27.05
Atenolol hcl	−1	−1.58	123.454	4	6.45	0.826794	−0.42	266.336	−0.109	8	−2.5	84.58
Enalapril maleate	−1.72	−1.32	192.686	2	8.5	0.7973544	−0.257	376.4467	0.667	11	−0.55	95.94
Enprofylline	−0.77	−0.73	67.355	2	5	0.9271436	0.52	194.1906	0.396	2	0.27	83.54

[a] QikProp descriptors.

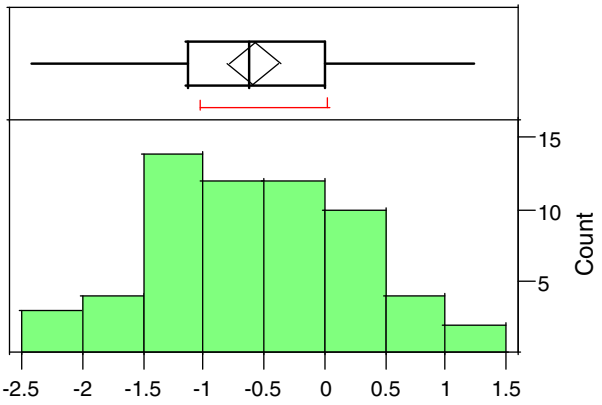

Figure 1. Distribution of the logarithm of experimental permeability values measured across Franz cell (cm/s).

solutes.[35,36] Polyethylene glycol (PEG 400) was used as the organic co-solvent (45% w/v) because its effect on skin permeability is minimal[37–39] and it is effective in boosting the solubility of lipophilic solutes.[40] To eliminate the need to normalize data for each cassette over many different skin sources, we included an internal reference standard, 3-isobutyl-1-methylxanthine (IBMX) in every cassette. Normalizing observed permeability coefficients against the reference standard in the same diffusion cell usually caused a significant reduction in variability.[39] Sufficient dose volume was used to maintain 'infinite dose' conditions so that permeability coefficients could be readily derived from the linear portion of the flux curves. From these studies, we have compiled a set of internally consistent permeability coefficients, suitable for developing quantitative models for human skin permeation.

The correlation of the skin permeability values with each of the four commonly used molecular descriptors is shown in Figure 2a–d. The measured permeabilities show weak correlation with TPSA, log *D*, and *C* log *P* and no correlation with the number of rotatable bonds of the molecule. These results are expected and consistent with earlier studies. Since our goal was to develop a simple model using as few descriptors as possible with accurate prediction and easy interpretation, we evaluated multiple linear regression models. To compare our models with the Potts and Guy's model shown in Eq. 1, we fit the Franz cell permeability data with the *C* log *P* and MW.

$$\log P_e = 0.2347 - 0.0055 * MW + 0.3865 * C\log P \quad (2)$$

This model has an $r^2 = 0.53$ and MAE = 0.44. We also obtained another model with the four parameters discussed above.

$$\log P_e = 0.1569 + 0.034 * C\log P - 0.0102 * \#rotor - 0.0144 * TPSA + 0.1321 * \log D \quad (3)$$

This model has an $r^2 = 0.60$ and MAE = 0.41. To improve the correlation with the experimental permeability data, we tried different sets of descriptors. We also wanted to publish the skin permeability model through Pfizer's global compchem toolbox for easy access and use by researchers within the company. Therefore we initially restricted our descriptor calculations to a single method—QikProp.[32] We have had prior success with developing QSAR models for various ADMET endpoints using QikProp descriptors.[41]

The model obtained by stepwise multiple regression method in JMP software that satisfied our simple criteria is shown below:

$$\log P_e = 6.6177 - 0.0022 * PISA - 0.3516 * \text{donorHB} - 0.2451 * \text{accptHB} - 5.8373 * \text{glob} + 0.2700 * \text{EA(eV)} \quad (4)$$

where PISA is the pi (carbon and attached hydrogen) component of the solvent-accessible surface area, donorHB is the estimated number of hydrogen bonds that would be donated by the solute in solution, accptHB is the estimated number of hydrogen bonds that would be accepted by the solute in solution, glob is the globularity descriptor and is equal to $4 * \pi * r^2/\text{SASA}$ where *r* is the radius of a sphere with a volume equal to the molecular volume and SASA is the solvent-accessible surface area (glob is equal to 1.0 for a spherical molecule), and EA(eV) is the quantum mechanically calculated electron affinity.[32]

This model gave a correlation coefficient, $r^2 = 0.77$ between experiment and prediction and the MAE of 0.3 for the set of 61 compounds. The cross validation with 'leave 20% out' method shows $q^2 = 0.71$ with the MAE of 0.34. The correlation of permeability values between experiment and prediction is shown in Figure 3. From the model we interpret that the factors that impact skin permeability are hydrogen bonding capabilities, molecular shape (globularity), pi system of the compound, and electron affinity, all of which make sense. To assess the level of contribution of each descriptor to skin permeability, we obtained a new model based on the normalized descriptors (mean center and scaling the untransformed descriptors using the caret package in R-http://www.R-project.org).

$$\log P_e = -0.7744 - 0.4276 * \text{PISA} - 0.7032 * \text{donorHB} - 1.0111 * \text{accptHB} - 0.4868 * \text{glob} + 0.3004 * \text{EA(eV)} \quad (5)$$

This equation provides the level of contribution and importance of different descriptors: hydrogen bond acceptor > hydrogen bond donor > globularity > PISA > electron affinity.

Previously published predictive models (e.g., Potts and Guy[3]) suggest that lipophilicity and size are the most important properties governing skin permeation. The model presented here is unique in that neither of these properties is used even though these two parameters from QikProp were considered in model building. It is important to realize that the vehicle used for permeation in all published models is water. While a 100% aqueous vehicle is the most appropriate standard state, such a vehicle does not represent typical topical discovery project applications.

The minimal impact of lipophilicity in our model is probably a consequence of the 40% PEG 400 in the vehicle. Lipophilicity as a driving force is largely a consequence of the unusual cohesive energy density of water[42] (as indicated by the surface tension). The energetic cost of creating a solute-sized cavity in water is higher than in most other phases, thus driving the solute into the more receptive phase. The presence of PEG significantly reduces surface tension, so that it may not be very different between the vehicle and the barrier phase. As a result, lipophilicity loses importance.

In considering the role of solute size in skin permeation, while overall size was not a major factor in our model, solute bulkiness, as measured by the globularity term (glob), was significant. The negative effect of globularity may reflect narrow pathways within the intercellular lipid phase of the stratum corneum through which a skin-permeating solute must pass.

Previous models often show a significant negative influence of hydrogen bond acceptor ability on solute permeation. Solute acceptor ability decreases partitioning from water into the barrier phase, because the H-bond donor capacity of water is much greater than that of the barrier phase. Solute H-bond donor capacity appears to be less important in governing permeation through skin because, with respect to partitioning, the acceptor capacity of the barrier phase and of the aqueous vehicle is similar. In our studies, the presence of PEG 400 in the vehicle will reduce the relative H-bond donor capacity of the vehicle.[43] Consequently, the H-bond acceptor capacity of the solute becomes somewhat less of a factor

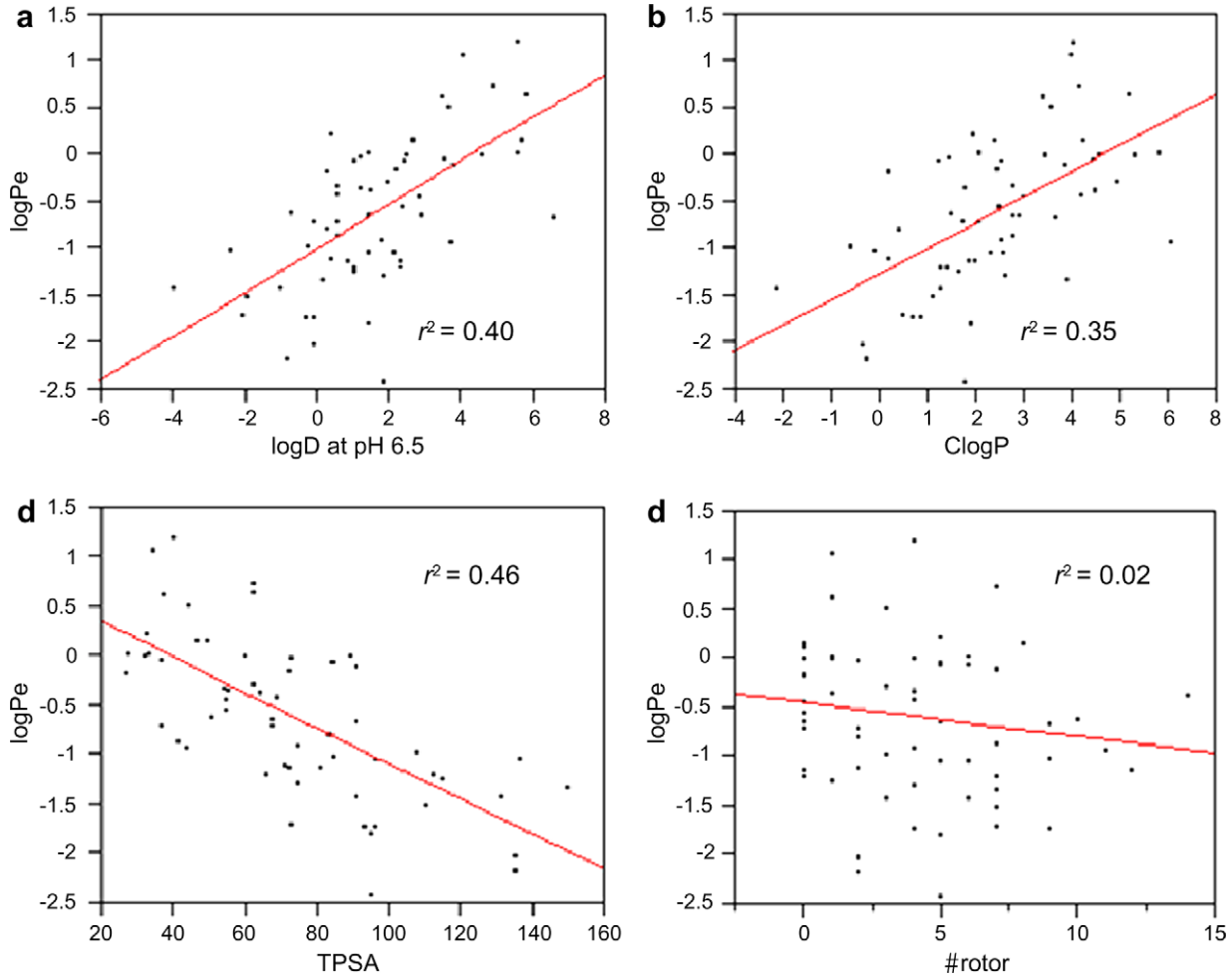

Figure 2. (a) Correlation of log P_e, (b) correlation of log P_e with C log P with log D at PH 6.5. (c) Correlation of log P_e **2d**. (d) Correlation of log P_e with TPSA with rotatable bonds.

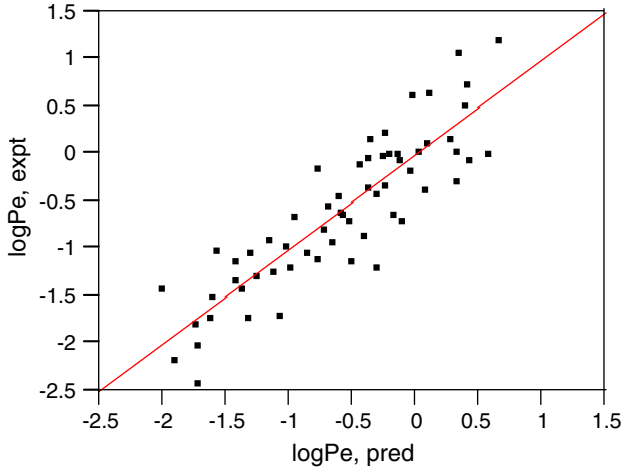

Figure 3. Correlation of permeability between experimental values and predicted values.

than it would be in a completely aqueous vehicle. Nevertheless, both acceptor and donor capacity of the solute will contribute to slowing down diffusion through the barrier phase. Thus, in our model, both donor and acceptor capacity of solutes is important, although acceptor capacity is still the most important.

Ionization would be expected to be a major factor in determining skin permeation, although it has rarely been incorporated explicitly into predictive models.[44] Acidic and basic solutes will have various degrees of ionization depending on the vehicle pH. We arbitrarily chose a pH of 6.4 for our studies, midway between the pH of plasma and that of the skin surface. The importance of the electron affinity term (EA(ev)) may be partially a consequence of solute ionization. High electron affinity is a characteristic of a (Lewis) acid. A positive correlation of solute permeation with this term could suggest that acids are preferentially permeable. This possibility should be tempered, however, with the observation that at pH 6.4, typical acids are less ionized than typical bases, so any apparent advantage of acidity may only be an indication of a lower percent ionization. In fact another study (unpublished) suggests that strong bases are more skin-permeable than strong acids.

There are several ways in which the use of cassettes could result in erroneous flux data. These can be summarized as solute–skin interactions and solute–solute interactions. Interaction of a solute with skin could potentially alter the skin barrier properties, resulting in greater or lesser apparent permeation for companion solutes. The relatively low concentration of individual solutes compared to what is typically used for permeation enhancers reduces this effect. Indeed, several studies with potential enhancers at ~0.1% concentration suggested that barrier alteration was minimal.[39] Solute–solute interactions in the vehicle could reduce the

thermodynamic activity of a solute so that activity is not properly reflected by the concentration. This is important, because solute concentration is used in calculating permeability coefficients. The use of buffer with 45% PEG 400 (w/v) should reduce, but may not eliminate solute–solute interaction in the vehicle. Solute–solute interaction in the barrier phase is also a possibility. High local concentrations of solutes at interfacial sites potentially could promote complexation resulting in altered permeation. However, studies of several pairs of solutes, singly and together, did not show evidence of interactions.[35]

In most cases, variation in measured solute permeability coefficients was reduced when the values were normalized against the IBMX permeability coefficient. Nevertheless, in some cases normalization had no effect or even increased the standard deviation for a set of permeation measurements.[39] The most likely cause for such observations is differences in the rate-limiting step of diffusion between the test and reference solutes. For small hydrophilic compounds, a pore pathway across the stratum corneum may contribute to the flux, while for highly lipophilic compounds, rate-limiting flux across the viable epidermis/dermis becomes significant. Solutes for which normalization fails to reduce variability are generally quite lipophilic or hydrophilic.

Large internally consistent data sets are hard to obtain because skin permeability studies are so labor intensive. The difficulty is compounded by the necessity of using multiple skin sources per solute to average out permeability differences. While a 100% aqueous vehicle is the most appropriate standard state, such a vehicle does not represent what is typical in topical discovery project applications. Here we have presented both the generation of a consistent data-set and the development of a computational skin permeability model used in our discovery efforts. The QSAR model contained only five simple descriptors and had a correlation coefficient, $r^2 = 0.77$ between experimental and calculated values. The MAE was 0.3 for the entire set and the cross validation coefficient, $q^2 = 0.71$ The model was used to both prioritize compounds that went through the Franz cell skin permeability assay as well as a computational filter for virtual library design and in the optimization of skin permeabilities of compounds in several dermatology projects.

Supplementary data

Supplementary data associated with this article can be found, in the online version, at doi:10.1016/j.bmcl.2009.11.039.

References and notes

1. Berner, B.; Cooper, E. R. *Transderm. Delivery Drugs* **1987**, *2*, 41.
2. Lian, G.; Chen, L.; Han, L. *J. Pharm. Sci.* **2007**, *97*, 584.
3. Potts, R. O.; Guy, R. H. *Pharm. Res.* **1992**, *9*, 663.
4. Inglese, M. J.; Fleischer, A. B., Jr.; Feldman, S. R.; Balkrishnan, R. *J. Dermatol. Treat.* **2008**, *19*, 27.
5. Jalian, H. R.; Takahashi, S.; Kim, J. *Comp. Med. Chem. II* **2006**, *7*, 935.
6. Sawaya, M. E. *Expert Opin. Ther. Pat.* **1997**, *7*, 859.
7. Shahi, S.; Athawale, R.; Ghadge, S. *SOFW J.* **2008**, *134*, 2.
8. Le Joliff, J.-C. *Actual. Chim.* **2006**, *299*, 12.
9. Roseborough Ingrid, E.; Grevious Mark, A.; Lee Raphael, C. *J. Natl. Med. Assoc.* **2004**, *96*, 108.
10. Bouwstra, J. A.; Honeywell-Nguyen, P. L. *Adv. Drug Delivery Rev.* **2002**, *54*, S41.
11. Menton, D. N.; Eisen, A. Z. *J. Ultrastruct. Res.* **1971**, *35*, 247.
12. Holbrook, K. A.; Odland, G. F. *J. Invest. Dermatol.* **1974**, *62*, 415.
13. Amsden, B. G.; Goosen, M. F. A. *AIChE J.* **1995**, *41*, 1972.
14. Fiserova-Bergerova, V.; Pierce, J. T.; Droz, P. O. *Am. J. Ind. Med.* **1990**, *17*, 617.
15. McKone, T. E.; Howd, R. A. *Risk Anal.* **1992**, *12*, 543.
16. Moss, G. P.; Dearden, J. C.; Patel, H.; Cronin, M. T. D. *Toxicol. In Vitro* **2002**, *16*, 299.
17. Anderson, B. D.; Raykar, P. V. *J. Invest. Dermatol.* **1989**, *93*, 280.
18. Cleek, R. L.; Bunge, A. L. *Pharm. Res.* **1993**, *10*, 497.
19. Abraham, M. H.; Martins, F.; Mitchell, R. C. *J. Pharm. Pharmacol.* **1997**, *49*, 858.
20. Buchwald, P.; Bodor, N. *J. Pharm. Pharmacol.* **2001**, *53*, 1087.
21. Pugh, W. J.; Hadgraft, J.; Roberts, M. S. *Drug Pharm. Sci.* **1998**, *91*, 245.
22. Lim, C. W.; Fujiwara, S.-I.; Yamashita, F.; Hashida, M. *Biol. Pharm. Bull.* **2002**, *25*, 361.
23. Frasch, H. F. *Risk Anal.* **2002**, *22*, 265.
24. Kasting, G. B.; Smith, R. L.; Cooper, E. R. *Pharmacol. Skin* **1987**, *1*, 138.
25. Cronin, M. T. D. *Dermal. Absorp. Model Toxicol. Pharmacol.* **2006**, 113.
26. Cronin, M. T. D.; Schultz, T. W. *THEOCHEM* **2003**, *622*, 39.
27. Flynn, G. L. In *Principles of Route-to-route Extrapolation for Risk Assessment*; Gerity, T. R., Henry, C. J., Eds.; Elsevier: Amsterdam, 1990; p 93.
28. Corina Version 3.1, Molecular Networks Gmbh, Germany.
29. *C* log *P* Version 4.3, Biobyte Corp.
30. Ertl, P.; Rohde, B.; Selzer, P. *J. Med. Chem.* **2000**, *43*, 3714.
31. JMP Version 5.0.1.2, SAS Institute, Cary, NC.
32. QikProp, Version 2.1, Schrödinger, New York.
33. Tan, C. Y.; Iglewicz, B. *Technometrics* **1999**, *41*, 192.
34. All Franz diffusion cell studies were conducted using a MicroettePlus™ System (Hanson Research, C., CA). This is an automated system for diffusion cell studies, permitting unattended sample collection at programed time intervals. The collection method removes about half of the total receiver volume at each sampling time. The Franz vertical diffusion cells (4 ml receiver volume, 0.64 cm^2 barrier surface areas) are water jacketed, allowing temperature control by a recirculating water bath. For these studies, cell temperature was 32 °C. Diffusion experiments were carried out over 48 h permitting (in most cases) attainment of steady state. Dose solutions consisted of cassettes of five compounds, one of these being the reference standard, IBMX. 1 mg of each compound per ml of vehicle was used. The vehicle was 45% PEG 400 (J.T.Baker)/65% phosphate buffered saline (PBS) (Gibco™) (w/v) with 15 mM MES buffer added to the PBS and adjusted to pH 6.4 with NaOH solution. Readjustment of pH was frequently necessary after dissolving solutes. Solute that did not dissolve was filtered out with GHP Acrodisc® 13 mm syringe filters, 0.45 μm pore size (PALL Life Sciences, East Hills, NY). Actual solute solution concentrations in dose solutions were determined by HPLC. A large dose volume (1 ml) with occlusion was used to prevent changes in the vehicle composition over time. The receiver solution was PBS with 0.1% Brij 98 (to reduce solute adsorption to glass) and 1 mM NaN_3 (to control bacterial growth; we now prefer 10 μg/ml gentamicin). Receiver solution was degassed by vacuum filtration at ~40 °C. Dermatomed human female back skin (0.4–1.1 mm), obtained from cadavers (U.S. Tissue & Cell, Cincinnati, OH) was used as the permeation barrier. For each cassette, two diffusion cells were used with each of two skin donors, yielding a total of 4 cells per cassette. Typically, 4 cassettes (16 cells) were run at one time, so that permeability coefficients for 16 compounds and the reference compound were determined in each study. After adding dose solution to each Franz cell, receiver solution samples were collected at 0.25, 4, 10, 16, 24, 32, 40 and 48 h. The 0.25 h sample was used as *t*0. The concentration of solutes in these samples was determined by LC/MS/MS. The cumulative mass of solute transferred was calculated at each time point and plotted against time. Mass transfer per unit time was calculated from the linear portion of the curve, usually in the second 24 h. Permeability coefficients were calculated as the quotient of the flux and the solute concentration in the donor solution. Normalized permeability was calculated as the mean of the ratio of the permeability coefficient of the solute and the permeability coefficient of IBMX determined in the same Franz cell. Data from cells in which obvious leakage occurred was not included in the mean. Solute concentrations in the dose solution were measured by HPLC to avoid inherent problems with mass spectrometry caused by PEG 400. Chromatography was done with an Agilent 1100 modular HPLC system (Agilent Technologies, Palo Alto, CA), using the G1315B diode-array detector. A Chromolith™ SpeedRod RP18e (50 × 4.6 mm) (Merck KGaA, Darmstadt, Germany) with concentration gradient (5–90% CH_3CN) and flow gradient (0.4–4 ml/min) was used. Use of a monolithic column enabled the determination of compounds with a broad range of lipophilicity in a run time of 7.5 min. Solute concentrations in the receiver solutions were determined using LC/MS/MS. Typically, analysis was carried out using a high-performance liquid chromatography system consisting of a Shimadzu binary pump (Shimadzu Scientific Instruments, Columbia, MD) with CTC PAL autosampler (Leap Technologies, Carrboro, NC) interfaced to an API 3000 or API 4000 LC/MS/MS quadrupole tandem mass spectrometer (Applied Biosystems/ MDS Sciex Inc., Ontario, Canada). The chromatography employed a short reversed phase column, for example, a Hypersil C18 Gold column (2.1 × 50 mm, 5 μm), and elution with a fast gradient from 10% to 90% acetonitrile. Flow rate was 0.3 ml/min and run time was 3 min. Detection was usually done with positive ion ESI mode, except for compounds where negative ion ESI mode was significantly more sensitive. All raw data was processed using Analyst Software ver. 1.4 (Applied Biosystems/ MDS Sciex Inc., Ontario, Canada).
35. Connors, K. A.; Khossravi, D. *J. Soln. Chem.* **1993**, *22*, 677.
36. Kristiansen, H.; Nakano, M.; Nakano, N. I.; Higuchi, T. *J. Pharm. Sci.* **1970**, *59*, 1103.
37. Catz, P.; Friend, D. R. *Int. J. Pharm.* **1990**, *58*, 93.
38. Cho, A.-R. *J. Korean Pharm. Sci.* **1996**, *26*, 99.
39. Conradi, R.A., unpublished results.
40. Rytting, E.; Lentz, K. A.; Chen, X.-Q.; Qian, F.; Venkatesh, S. *AAPS J.* **2005**, *7*, E78.
41. Lee, P. H., Shanmugasundaram, V., unpublished results.
42. Sinanoglu, O. *J. Chem. Phys.* **1981**, *75*, 463.
43. Kim, I.-W.; Jang, M. D.; Ryu, Y. K.; Cho, E. H.; Lee, Y. K.; Park, J. H. *Anal. Sci.* **2002**, *18*, 1357.
44. Abraham, M. H.; Martins, F. *J. Pharm. Sci.* **2004**, *93*, 1508.